IOP Publishing Journal of Physics B: Atomic, Molecular and Optical Physics
J. Phys. B: At. Mol. Opt. Phys. **49** (2016) 094004 (6pp) doi:10.1088/0953-4075/49/9/094004

Grover search algorithm with Rydberg-blockaded atoms: quantum Monte Carlo simulations

David Petrosyan[1], **Mark Saffman**[2] **and Klaus Mølmer**[3]

[1] Institute of Electronic Structure and Laser, FORTH, GR-71110 Heraklion, Crete, Greece
[2] Department of Physics, University of Wisconsin-Madison, Madison, Wisconsin 53706, USA
[3] Department of Physics and Astronomy, Aarhus University, DK-8000 Aarhus C, Denmark

E-mail: dap@iesl.forth.gr

Received 21 December 2015
Accepted for publication 4 March 2016
Published 18 April 2016

Abstract

We consider the Grover search algorithm implementation for a quantum register of size $N = 2^k$ using k (or $k + 1$) microwave- and laser-driven Rydberg-blockaded atoms, following the proposal by Mølmer *et al* (2011 *J. Phys. B* **44** 184016). We suggest some simplifications for the microwave and laser couplings, and analyze the performance of the algorithm for up to $k = 4$ multilevel atoms under realistic experimental conditions using quantum stochastic (Monte Carlo) wavefunction simulations.

Keywords: quantum computation, quantum algorithms, Rydberg blockade, Grover search

(Some figures may appear in colour only in the online journal)

1. Introduction

Strong, long-range interactions between atoms in high-lying Rydberg states make them attractive systems for quantum information applications [1]. The interaction-induced level shifts suppress resonant optical excitation of Rydberg states of more than one atom within a certain blockade distance from each other [1, 2]. This blockade effect can then be used to implement quantum logic gate operations between closely spaced atoms [3–8], or to realize atomic ensemble qubits with Rydberg superatoms which can accommodate at most one collective Rydberg excitation at a time [9–13].

The Grover quantum search algorithm [14], which offers a quadratic speed-up of the search of unstructured databases over classical search algorithms, is a paradigmatic example of the power of quantum computation [15, 16]. The protocol consists of repeated application of the query (oracle) and inversion-about-the-mean (Grover) operations to a quantum register composed of k qubits which can store 2^k elements (database entries).

As any other quantum computation procedure, both the oracle and Grover operations can be implemented by a sequence of standard, universal one- and two-qubit gates [15]. When the number of qubits k increases beyond just a few, however, such implementations become quite complex and experimental demonstrations of the Grover search algorithm have so far been restricted to the case of $k = 2$ [17–20].

In contrast, an efficient procedure to implement the Grover search algorithm using the multi-atom interactions mediated by the Rydberg blockade was proposed in [21]. In that proposal, individual qubits are encoded in pairs of metastable states of single atoms trapped in an array of microtraps, and the oracle and Grover operations require only simple sequences of excitation and de-excitation processes between the qubit states and the Rydberg state in each atom. Here we suggest a practical implementation of this proposal with microwave and laser drivings of the atoms. We perform extensive numerical simulations of the dynamics of the system under realistic assumptions about the interatomic interaction strengths as well as atomic decay and dephasing parameters. We present results for the success probabilities of the Grover search with a moderate—but computationally non-trivial—register size of $k \leqslant 4$. We explore two different interaction configurations proposed in [21], wherein the blockade interaction is present either between any pair of register atoms excited to the Rydberg state, or only between

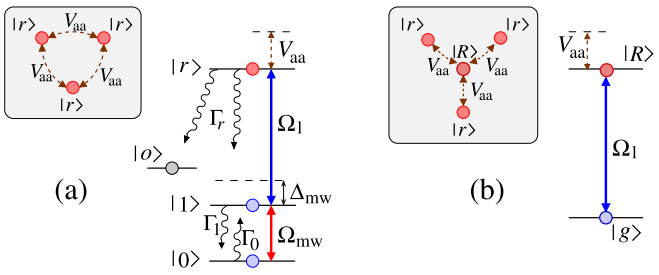

Figure 1. (a) Level scheme of the register atoms interacting with a microwave field on the transition $|0\rangle \leftrightarrow |1\rangle$ with Rabi frequency Ω_{mw}, and with resonant laser field(s) on the transition $|1\rangle \leftrightarrow |r\rangle$ with Rabi frequency Ω_l. The coupling of selected atoms with the global microwave field can be made resonant ($\Delta_{mw} \ll |\Omega_{mw}|$) or strongly detuned ($\Delta_{mw} \gg |\Omega_{mw}|$). State $|o\rangle$ accounts for the loss of the atom due to decay from $|r\rangle$ to any other state but $|0\rangle$ or $|1\rangle$. Inset: atoms in Rydberg states $|r\rangle$ interact with each other via a strong, long-range potential $V_{aa} \gg |\Omega_l|$ which suppresses Rydberg excitation of all but one atom at a time. (b) Level scheme of an ancilla atom whose transition $|g\rangle \leftrightarrow |R\rangle$ is driven by a focused resonant laser with Rabi frequency Ω_l. Inset: the ancilla atom in Rydberg state $|R\rangle$ interacts with all the $|r\rangle$-state register atoms via the strong potential V_{aa}, while the register atoms do not directly interact with each other.

an auxiliary atom and each register atom. Both configurations have advantages and disadvantages for the experimental realization, and we find that they yield similar performance of the algorithm.

2. The atomic system

Consider k atoms with the level scheme sketched in figure 1(a). States $|0\rangle$ and $|1\rangle$ of each atom are the qubit basis states. A time-dependent microwave field acts on the transition $|0\rangle \leftrightarrow |1\rangle$ with the Rabi frequency $\Omega_{mw}(t) = |\Omega_{mw}|e^{i\phi}$ having real amplitude $|\Omega_{mw}|$ and phase ϕ. The corresponding Hamiltonian for the jth atom is

$$H_{mw}^{(j)} = -\hbar\,[\Delta_{mw}^{(j)}\sigma_{11}^{(j)} + \frac{1}{2}\Omega_{mw}\sigma_{10}^{(j)} + \frac{1}{2}\Omega_{mw}^{*}\sigma_{01}^{(j)}], \qquad (1)$$

where $\sigma_{\mu\nu}^{(j)} \equiv |\mu\rangle_j\langle\nu|$ are the atomic operators, and $\Delta_{mw}^{(j)}$ is the microwave field detuning.

A resonant field, $\Delta_{mw} = 0$, applied to the atom leads to the unitary transformation (in the qubit basis $\{|0\rangle, |1\rangle\}$)

$$U_\phi(\theta) = \begin{bmatrix} \cos\frac{1}{2}\theta & ie^{-i\phi}\sin\frac{1}{2}\theta \\ ie^{i\phi}\sin\frac{1}{2}\theta & \cos\frac{1}{2}\theta \end{bmatrix}, \qquad (2)$$

where $\theta = \int|\Omega|dt$ is the pulse area [16]. Hence, $\theta = \pi$ with $\phi = 0$ $(\pi/2)$ corresponds to the iX (iY) operation on the qubit [15]. The Z gate can be realized as $U_{\pi/2}(\pi)U_0(\pi) = iZ$, which, for a fixed maximum amplitude of $|\Omega|$, takes twice the time of the X or Y gate. The Hadamard gate can be realized as $U_{\pi/2}(\pi/2)U_0(\pi) = iH$, which takes 1.5 times longer than X or Y. In what follows, we will only use the operations $U_0(\pi) = iX$ and the Hadamard-like $U_{\pm\pi/2}(\pi/2)$ which takes only half the time of X.

Since the distance between the atoms is small—of the order of a few μm [5–8] for the Rydberg blockade to be effective (see below)—the microwave field with a long wavelength of several cm affects all the atoms with the same Rabi frequency. We assume that the frequency of the microwave field can be tuned into, or detuned from, the transition resonance $|0\rangle \leftrightarrow |1\rangle$ of the unperturbed atoms. In addition, we assume that using focused, non-resonant laser beams we can induce ac Stark-shifts of e.g., state $|1\rangle$ of the selected atoms to make the transition $|0\rangle \leftrightarrow |1\rangle$ resonant with the microwave field (when it is non-resonant otherwise), or to detune it by a large amount $\Delta_{mw} \gg |\Omega_{mw}|$ (when it is resonant otherwise) [22]. We can therefore selectively couple or decouple the atoms to and from the global microwave field.

Each register atom j in state $|1\rangle$ can be excited by a focused laser beam to a Rydberg state $|r\rangle$, see figure 1(a). This process is described by the Hamiltonian

$$H_l^{(j)} = -\hbar\frac{1}{2}[\Omega_l^{(j)}\sigma_{rl}^{(j)} + \Omega_l^{*(j)}\sigma_{lr}^{(j)}], \qquad (3)$$

were $\Omega_l^{(j)}$ is the Rabi frequency, and we assume that the laser is resonant for an unperturbed (not blockaded) atom, leading to the same transformations as in equation (2) between states $|1\rangle$ and $|r\rangle$. We will also employ an auxiliary (ancilla) atom a with levels $|g\rangle$ and $|R\rangle$ similarly coupled by a focused resonant laser, as shown in figure 1(b).

As in [21], we will consider two possible scenarios of interatomic interactions. In the first case (see the inset of figure 1(a)), any pair of register atoms i and j in state $|r\rangle$ interact with each other via the long-range potential

$$H_{aa}^{(i,j)} = \hbar\frac{C_p}{|\mathbf{r}_i - \mathbf{r}_j|^p}\sigma_{rr}^{(i)} \otimes \sigma_{rr}^{(j)}, \qquad (4)$$

where $\mathbf{r}_{i,j}$ are the atomic positions, and $p = 3$ or 6 for the dipole–dipole or van der Waals interactions, respectively [1]. If the interaction-induced level shifts $V_{aa} = C_p/r_{ij}^p$ are large enough, then an atom already excited to the Rydberg state $|r\rangle$ will block subsequent excitation of all the other atoms. In the second case (see the inset of figure 1(b)), we assume that the register atoms do not interact with each other, but each register atom j in state $|r\rangle$ interacts with the ancilla atom a in state $|R\rangle$ via the potential

$$H_{aa}^{(j,a)} = \hbar\frac{C_p}{|\mathbf{r}_j - \mathbf{r}_a|^p}\sigma_{rr}^{(j)} \otimes \sigma_{RR}^{(a)}, \qquad (5)$$

which can block the Rydberg excitation of the ancilla atom in the presence of one or more $|r\rangle$-state register atoms. This situation occurs for example for certain configurations of Rydberg excited states in rubidium and cesium [23].

We shall include in our treatment realistic atomic decay and dephasing, leading to decoherence and loss of atoms which strongly affect the outcome of the quantum computation. The atoms are subject to the following relaxation processes: slow decays of level $|1\rangle$ to $|0\rangle$ with rate Γ_1 and level $|0\rangle$ to $|1\rangle$ with rate Γ_0 [22]; the much faster decay of the Rydberg state $|r\rangle$ with rate $\Gamma_r = \Gamma_{r0} + \Gamma_{r1} + \Gamma_{ro}$ which has three contributions: the decay to $|0\rangle$, to $|1\rangle$ and loss of population to any other state represented in our model by $|o\rangle$ [8]; finally, we include dephasing γ_z on the qubit microwave

transition $|0\rangle \leftrightarrow |1\rangle$ and the typically much stronger dephasing γ_r of the atomic polarization on the optical transition $|1\rangle \leftrightarrow |r\rangle$ due to, e.g., the laser phase fluctuations, external field noise, and residual decay to $|1\rangle$ via a non-resonant intermediate excited state $|e\rangle$ (relevant, when $|1\rangle \leftrightarrow |r\rangle$ is a two-photon transition via $|e\rangle$). The corresponding Lindblad generators [15, 16] for the decay and dephasing processes are $L_{01}^{(j)} = \sqrt{\Gamma_0}\,\sigma_{10}^{(j)}$, $L_{10}^{(j)} = \sqrt{\Gamma_1}\,\sigma_{01}^{(j)}$, $L_{r0}^{(j)} = \sqrt{\Gamma_{r0}}\,\sigma_{0r}^{(j)}$, $L_{r1}^{(j)} = \sqrt{\Gamma_{r1}}\,\sigma_{1r}^{(j)}$, $L_{ro}^{(j)} = \sqrt{\Gamma_{ro}}\,\sigma_{or}^{(j)}$, and $L_{\rm mw}^{(j)} = \sqrt{\gamma_z/2}\,(2\sigma_{11}^{(j)} - \mathbb{1}^{(j)})$, $L_{\rm opt}^{(j)} = \sqrt{\gamma_r/2}\,(2\sigma_{rr}^{(j)} - \mathbb{1}^{(j)})$, where $\mathbb{1}^{(j)} \equiv \sum_\mu \sigma_{\mu\mu}^{(j)}$ is the unity operator for atom j.

For an isolated atom, the excitation linewidth of the Rydberg state $|r\rangle$ (from state $|1\rangle$) is $w = |\Omega_{\rm l}|\sqrt{\gamma_{r1}/\Gamma_r}$, where $\gamma_{r1} \equiv \frac{1}{2}(\Gamma_1 + \Gamma_r) + \gamma_r$ and $|\Omega_{\rm l}|^2 \gg \Gamma_r\gamma_{r1}$ [16]. In what follows, we position the atoms such that the interaction-induced level shifts $V_{\rm aa} \geqslant 10w$ are sufficiently large for the Rydberg blockade of any pair of register atoms i, j, or any register atom j and ancilla atom a.

3. The search algorithm implementation

With the Grover algorithm, we search for one particular marked element $x_m = b_0 b_1 \cdots b_{k-1}$ ($b_j \in [0, 1]$) in a database containing $N = 2^k$ elements $x = 00\cdots0,\ 00\cdots1,\ \ldots,\ 11\cdots1$. The algorithm consists of the following steps [14–16]:

(0) prepare the k-qubit register in an equally-weighted superposition $|s\rangle \equiv \left[\frac{|0\rangle + |1\rangle}{\sqrt{2}}\right]^{\otimes k} = \frac{1}{\sqrt{N}}\sum_x |x\rangle$ of all N possible states $|x\rangle$;

(1) apply to the register the oracle query operation which shifts the phase of state $|x_m\rangle = |b_0 b_1 \cdots b_{k-1}\rangle$ by π (flips the sign of c_{x_m}) relative to all the other states $|x\rangle$ of the superposition $\sum_{x=00\ldots0}^{11\ldots1} c_x\,|x\rangle$;

(2) apply to the register the inversion about the mean (Grover) operation.

The register preparation step (0) is applied only once. The combined effect of steps (1) and (2) is to increase the amplitude c_{x_m} of state $|x_m\rangle$ by $\sim 1/\sqrt{N}$ at the expense of amplitudes c_x of all the other states $|x\rangle$. Steps (1) and (2) are thus applied repeatedly, $\sim\sqrt{N}$ times, until the probability of the marked state approaches unity, at which time it is measured.

We now examine in some detail the implementation of each of the above steps, along the lines of the proposal of [21] with a view of possible experimental realization [8, 22].

(0) The register preparation step in [21] is performed in the standard way by applying the Hadamard gate H to all the register atoms initially in state $|0\rangle$. The resonant microwave implementation of H would involve $\pi + \pi/2$ pulses which take 1.5 times the duration of the X gate, but the initial superposition state can also be obtained by the shorter transformation $U_{-\pi/2}(\pi/2)$ applied *simultaneously* to all the atoms (qubits) in state $|0\rangle$: $U_{-\pi/2}(\pi/2)\,|0\rangle \to [\,|0\rangle + |1\rangle\,]/\sqrt{2}$.

(1) In the oracle step, the protocol of [21] applies sequentially to each register atom $j = 0, 1, \ldots, k-1$ a π-pulse $U_0(\pi)$ between states $|1 - b_j\rangle$ and $|r\rangle$ using focused laser beams; if any one atom is transferred to $|r\rangle$, then all the subsequent atoms remain in their initial state $|0\rangle$ or $|1\rangle$ due to the Rydberg blockade (assuming the interaction scenario of equation (4)). This is then followed by the same operation $U_0(\pi)$ on all the register atoms in the reverse order to bring the atom in Rydberg state $|r\rangle$ back to its initial state. The result of this transformation is that any state of the register $|\mu_0\mu_1\cdots\mu_{k-1}\rangle$ ($\mu = 0, 1$) having one or more digits different from the marked state $|b_0 b_1\cdots b_{k-1}\rangle$ will undergo one (and not more than one, due to the Rydberg blockade) full Rabi cycle via the Rydberg state and accumulate a π phase shift, while only the marked state $|b_0 b_1\cdots b_{k-1}\rangle$ will remain unchanged.

We now assume that the Rydberg exciting lasers with fixed frequency act only on the transition $|1\rangle \to |r\rangle$. We should therefore implement the oracle step by applying first the $b_j X$ transformation to each register atom, which flips the qubit states $|0\rangle$ and $|1\rangle$ if $b_j = 1$ and does nothing otherwise, and then apply the Rydberg excitation and de-excitation lasers, followed again by the $b_j X$. To implement the $b_j X$ with our setup, we apply the global microwave $U_0(\pi) = \mathrm{i}X$ pulses to all the atoms *simultaneously*, but we use Stark lasers to adjust each atom's detuning with respect to the microwave frequency to $(1 - b_j)\Delta_{\rm mw}$, respectively [22].

(2) In the Grover step, [21] proposes to transfer sequentially each register atom in state $[\,|0\rangle - |1\rangle\,]/\sqrt{2}$ to the Rydberg state $|r\rangle$ and then back in reverse order, while leaving the atoms in the 'dark' state $[\,|0\rangle + |1\rangle\,]/\sqrt{2}$ unaffected by the Rydberg lasers. Again, Rydberg excitation of any one atom would block subsequent excitation of the other atoms (assuming the interactions of equation (4)). This transformation leaves the equally-weighted superposition state $|s\rangle$ unchanged, while flipping the sign of all the other orthogonal states of the register, which results in the inversion about the mean operation [14–16].

We implement this Grover operation by first applying to all the atoms *simultaneously* the microwave $U_{\pi/2}(\pi/2)$ pulse which results in transformation

$$U_{\pi/2}(\pi/2)[\,|0\rangle + |1\rangle\,]/\sqrt{2} \to |0\rangle,$$
$$U_{\pi/2}(\pi/2)[\,|0\rangle - |1\rangle\,]/\sqrt{2} \to -|1\rangle.$$

We then apply the resonant Rydberg excitation and de-excitation lasers on the transition $|1\rangle \to |r\rangle$. Finally, we apply to all the atoms *simultaneously* the microwave $U_{-\pi/2}(\pi/2)$ pulse which leads to

$$U_{-\pi/2}(\pi/2)\,|0\rangle \to [\,|0\rangle + |1\rangle\,]/\sqrt{2},$$
$$U_{-\pi/2}(\pi/2)(-|1\rangle) \to [\,|0\rangle - |1\rangle\,]/\sqrt{2},$$

as was required.

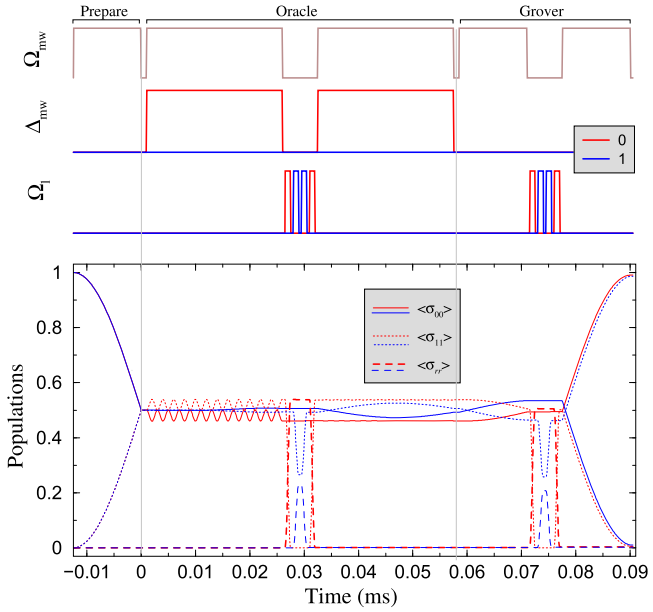

Figure 2. Time-dependence of the microwave and laser fields (top) acting on atoms $j = 0, 1$ (see the legend for color code), and populations $\langle\sigma^{(j)}_{\mu\mu}\rangle$ of states $|\mu = 0, 1, r\rangle$ of the corresponding atoms (main panel), for one iteration of the search algorithm in a quantum register of $k = 2$ atoms interacting via equation (4). The marked input is $b_0 b_1 = 01$.

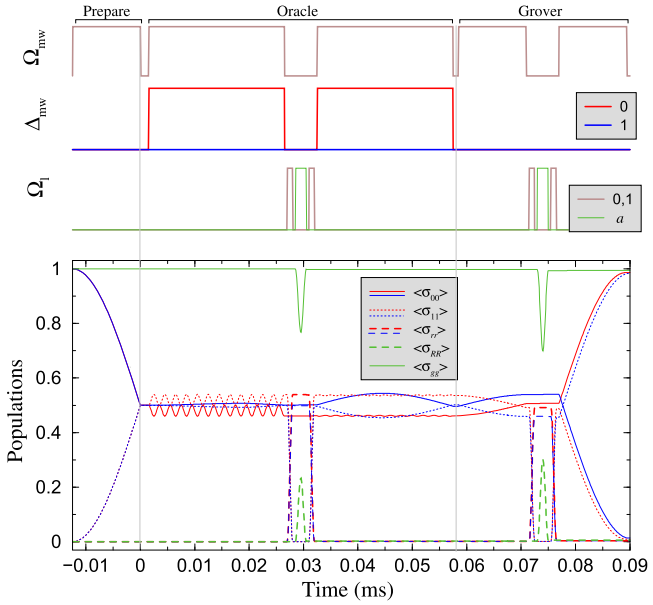

Figure 3. Same as in figure 2, but with ancilla atom a interacting with register atoms $j = 0, 1$ via equation (5).

In both steps (1) and (2) above, the conditional logic operations rely on the Rydberg blockade. In the interaction scenario of equation (4) (i.e., any pair of register atoms in state $|r\rangle$ strongly interact with each other), we apply the Rydberg excitation laser π-pulses $U_0(\pi)$ between states $|1\rangle$ and $|r\rangle$ sequentially to atoms $j = 0, 1, \ldots, k-1$, followed by the same de-excitation π-pulses $U_0(\pi)$ applied to the atoms in the reverse order $j = k-1, k-2, \ldots, 0$ [21]. In the experimentally slightly simpler case of interaction of equation (5) involving an ancilla atom (i.e., any register atom in state $|r\rangle$ interacts only with the ancilla atom blocking its excitation to state $|R\rangle$), we can apply the Rydberg excitation laser π-pulse $U_0(\pi)$ to all the register atoms j *simultaneously*, transferring any atom in state $|1\rangle$ to state $|r\rangle$. We then apply a 2π-pulse $U_0(2\pi)$ to the ancilla atom on the transition $|g\rangle \leftrightarrow |R\rangle$: if one or more register atoms are in state $|r\rangle$, the ancilla atom will remain in state $|g\rangle$ due to the Rydberg blockade; and only if no register atom is in state $|r\rangle$, the ancilla atom will undergo a full Rabi cycle between states $|g\rangle$ and $|R\rangle$ resulting in the sign change of the state of the combined system consisting of the register atoms and the ancilla. We then apply *simultaneously* to all the register atoms the de-excitation laser π-pulse $U_\pi(\pi)$ with the opposite sign ($\phi_l = \pi$ phase) of the Rabi frequency Ω_l so as to avoid the sign change of state $|1\rangle$.

To illustrate the foregoing discussion, in figures 2 and 3 we plot the time-dependence of the microwave and laser pulses and the resulting coherent dynamics of populations of the atomic states. In these figures, we show one full iteration of the search algorithm with $k = 2$ register atoms (plus the ancilla in figure 3) and a representative marked input, assuming negligible relaxation rates.

4. Results of simulations

We simulate the dissipative dynamics of the system of k atoms using the quantum stochastic (Monte Carlo) wavefunctions method [16, 24]. Using realistic experimental parameters, we test various inputs $b_0 b_1 \cdots b_{k-1}$ and for each input generate many independent trajectories for the time-evolution of the wavefunction of the system.

We assume that after each run, the experimentalist performs a projective measurement of all the register atoms (qubits) onto state $|0\rangle$. Then the negative outcome of the measurement on some atom j (i.e. the atom is not in state $|0\rangle$) would lead the experimentalist to assume $b_j = 1$ (and the atom is in state $|1\rangle$), but the same measurement outcome would correspond also to atom j being lost all together (the atom is in state $|o\rangle$). Thus, if we average over all possible inputs, a loss of an atom still leads to correct measurement result half of the time. It is a special feature of our Rydberg blockade implementation of the search algorithm that if an atom is lost during the calculation, the oracle and Grover operations still apply correctly to the remaining string of qubits [25] .

In figures 4 and 5 we show the result of our simulations for the interaction configurations of figures 1(a) and (b) (equations (4) and (5)) without and with the ancilla atom, respectively. The probabilities of detecting the system in the correct marked state $|b_0 b_1 \cdots b_{k-1}\rangle$ are obtained upon averaging over many independent realizations (trajectories) of the numerical experiment. More precisely, for an input of say $b_0 b_1 b_2 = 010$ we calculate the probability of detecting the system in state $|\mu_0 = 0, \mu_1 \neq 0, \mu_2 = 0\rangle$ ($\mu \neq 0$ is either $\mu = 1$ or $\mu = o$).

In both figures 4 and 5 we obtain similar results; only for very strong decay of the Rydberg state corresponding to panels (c1, c2) the scheme with the ancilla atom performed

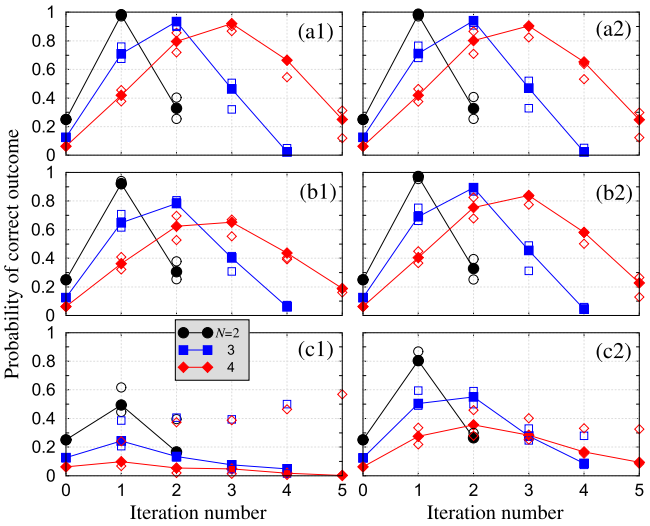

Figure 4. Probabilities of measuring correct outcomes $b_0 b_1 \cdots b_{k-1}$ of the Grover search versus number of iterations, for $k = 2, 3, 4$ digit register (black, blue, red, respectively) with the interaction scheme of figure 1(a) (equation (4)), obtained from averaging over 200 independent trajectories for the system wavefunction. The marked inputs for the filled symbols are 01, 010, 0101; other inputs, e.g., 00, 000, 0000 and 11, 111, 1111 shown with open symbols, lead to close results to within ±5% for (a1, a2, b1, b2), or are more divergent for (c1, c2) (typically, success probabilities for inputs 11, … are better than for 00, …, see the text for discussion). The Rabi frequency of the Rydberg excitation laser is $|\Omega_l| = 2\pi \times 0.5$ MHz in the left panels (a1, b1, c1) and $|\Omega_l| = 2\pi \times 2$ MHz in the right panels (a2, b2, c2). The Rydberg state decay is taken $\Gamma_r = (1, 4.76, 100) \times 10^3\ \mathrm{s}^{-1}$ in (a, b, c), respectively, with $\Gamma_{ro} = \frac{7}{8}\Gamma_r$ and Γ_{r0}, $\Gamma_{r1} = \frac{1}{16}\Gamma_r$. The dephasing rates on the Rydberg transitions are $\gamma_r = (1, 10, 100) \times 10^3\ \mathrm{s}^{-1}$ in (a, b, c), respectively. Other parameters, common to all the graphs, are Γ_0, $\Gamma_1 = 2\ \mathrm{s}^{-1}$, $\gamma_z = 100\ \mathrm{s}^{-1}$, $|\Omega_{\mathrm{mw}}| = 2\pi \times 20$ kHz (X gate time is 25 μs), and $\Delta_{\mathrm{mw}} = 25|\Omega_{\mathrm{mw}}|$, while the time interval between the gates is $\delta t = 50$ ns.

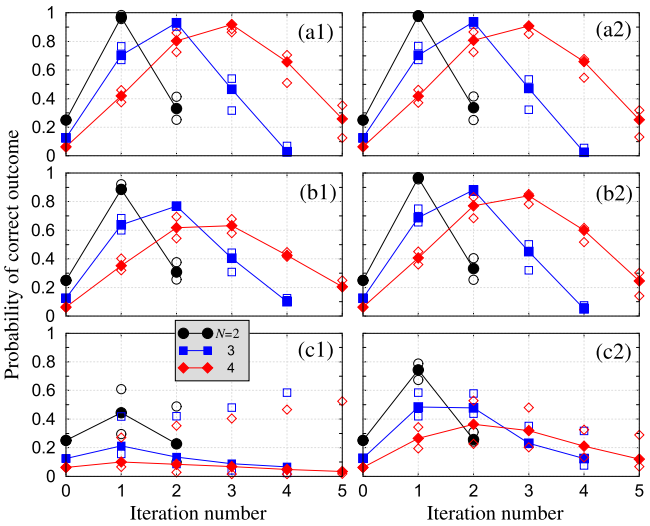

Figure 5. Same as in figure 4, but for the interaction scheme of figure 1(b) (equation (5)). Decay and dephasing of the ancilla atom are neglected.

somewhat worse, even though we neglected the decay and dephasing of the ancilla in figure 5 for a fair comparison with figure 4. This is due to the fact that the scheme with the ancilla permits multiple Rydberg excitations of the register atoms, leading to their larger aggregate probability of decay and loss.

We note that, for moderate values of the atomic decay and dephasing, digits $b_j = 0$ in the marked element tend to cause larger error in the outcome, because the microwave detuning $\Delta_{\mathrm{mw}} = 25|\Omega_{\mathrm{mw}}|$, which suppresses the X gate on atom j during the oracle operation, is large but still finite. More important are the relaxation processes which significantly degrade the performance of the algorithm with increasing evolution time. As a consequence, the probability for the correct measurement outcome may peak after fewer iterations than would be required to reach unity in the ideal case. It turns out that the errors due to the decay and dephasing on the qubit transition $|0\rangle \leftrightarrow |1\rangle$ play a minor role, despite the slowness of the operations performed by the microwave field with small Rabi frequency [22]. The larger decay rate $\Gamma_r \simeq 5\text{–}100 \times 10^3\ \mathrm{s}^{-1}$ and higher probability of atom loss from the Rydberg state [8] are more damaging, and the most harmful element is the large dephasing $\gamma_r = 10^5\ \mathrm{s}^{-1}$ of Rydberg transition. So either the laser Rabi frequency on the Rydberg transition should be increased, as in panels (a2, b2, c2) of figures 4 and 5, so that the decay and dephasing have less time to destroy the atomic coherences, or γ_r should be reduced. While for the dephasing rate γ_r we took a typical experimental value, there is no theoretical argument why this value could not be reduced by an order of magnitude or more.

5. Summary

To conclude, we have studied the Grover search algorithm implementation with several Rydberg blockaded atoms under realistic experimental conditions including the choice of parameters for the atomic decay, dephasing and interaction strengths. We have shown that relaxation processes cause decoherence during the quantum computation and reduce the probability of the correct outcome after a few iterations of the oracle and Grover steps.

The remarkable property of the Grover algorithm is that it can tolerate moderate amount of errors without error correction, with the measurement on the final state of the system still leading to increased probability of the sought-after element of the database. When the probability for the correct outcome is larger than all the probabilities for incorrect outcomes, one may have recourse to perform several experimental runs and measurements and obtain the correct result by a majority vote.

Acknowledgments

This work was supported by the US IARPA MQCO program, the EU H2020 FET-Proactive project RySQ, and the Villum Foundation.

References

[1] Saffman M, Walker T G and Mølmer K 2010 *Rev. Mod. Phys.* **82** 2313
[2] Comparat D and Pillet P 2010 *J. Opt. Soc. Am.* B **27** A208
[3] Jaksch D, Cirac J I, Zoller P, Rolston S L, Cote R and Lukin M D 2000 *Phys. Rev. Lett.* **85** 2208
[4] Isenhower L, Saffman M and Mølmer K 2011 *Quantum Inf. Process.* **10** 755
[5] Urban E, Johnson T A, Henage T, Isenhower L, Yavuz D D, Walker T G and Saffman M 2009 *Nat. Phys.* **5** 110
Isenhower L, Urban E, Zhang X L, Gill A T, Henage T, Johnson T A, Walker T G and Saffman M 2010 *Phys. Rev. Lett.* **104** 010503
[6] Gaëtan A, Miroshnychenko Y, Wilk T, Chotia A, Viteau M, Comparat D, Pillet P, Browaeys A and Grangier P 2009 *Nat. Phys.* **5** 115
Wilk T, Gaëtan A, Evellin C, Wolters J, Miroshnychenko Y, Grangier P and Browaeys A 2010 *Phys. Rev. Lett.* **104** 010502
[7] Beguin L, Vernier A, Chicireanu R, Lahaye T and Browaeys A 2013 *Phys. Rev. Lett.* **110** 263201
[8] Maller K M, Lichtman M T, Xia T, Sun Y, Piotrowicz M J, Carr A W, Isenhower L and Saffman M 2015 *Phys. Rev.* A **92** 022336
[9] Lukin M D, Fleischhauer M, Côté R, Duan L M, Jaksch D, Cirac J I and Zoller P 2001 *Phys. Rev. Lett.* **87** 037901
[10] Dudin Y O, Li L, Bariani F and Kuzmich A 2012 *Nat. Phys.* **8** 790
[11] Weber T M, Honing M, Niederprum T, Manthey T, Thomas O, Guarrera V, Fleischhauer M, Barontini G and Ott H 2015 *Nat. Phys.* **11** 157
[12] Ebert M, Kwon M, Walker T G and Saffman M 2015 *Phys. Rev. Lett.* **115** 093601
[13] Zeiher J, Schauß P, Hild S, Macri T, Bloch I and Gross C 2015 *Phys. Rev.* X **5** 031015
[14] Grover L K 1997 *Phys. Rev. Lett.* **79** 325
[15] Nielsen M and Chuang I 2000 *Quantum Computation and Quantum Information* (Cambridge: Cambridge University Press)
[16] Lambropoulos P and Petrosyan D 2007 *Fundamentals of Quantum Optics and Quantum Information* (Berlin: Springer)
[17] Chuang I L, Gershenfeld N and Kubinec M 1998 *Phys. Rev. Lett.* **80** 3408
[18] Brickman K-A, Haljan P C, Lee P J, Acton M, Deslauriers L and Monroe C 2005 *Phys. Rev.* A **72** 050306(R)
[19] Walther P, Resch K J, Rudolph T, Schenck E, Weinfurter H, Vedral V, Aspelmeyer M and Zeilinger A 2005 *Nature* **434** 169
[20] DiCarlo L *et al* 2009 *Nature* **460** 240
[21] Mølmer K, Isenhower L and Saffman M 2011 *J. Phys. B: At. Mol. Opt. Phys.* **44** 184016
[22] Xia T, Lichtman M, Maller K, Carr A W, Piotrowicz M J, Isenhower L and Saffman M 2015 *Phys. Rev. Lett.* **114** 100503
[23] Beterov I I and Saffman M 2015 *Phys. Rev.* A **92** 042710
[24] Dalibard J, Castin Y and Mølmer K 1992 *Phys. Rev. Lett.* **68** 580
Dum R, Zoller P and Ritsch H 1992 *Phys. Rev.* A **45** 4879
Gardiner C W, Parkins A S and Zoller P 1992 *Phys. Rev.* A **46** 4363
Plenio M B and Knight P L 1998 *Rev. Mod. Phys.* **70** 101
[25] Bhaktavatsala Rao D D and Mølmer K 2012 *Phys. Rev.* A **86** 042321